Acta Pharmaceutica Sinica B 2025;15(1):331−348

Chinese Pharmaceutical Association
Institute of Materia Medica, Chinese Academy of Medical Sciences

Acta Pharmaceutica Sinica B

www.elsevier.com/locate/apsb
www.sciencedirect.com

ORIGINAL ARTICLE

YOD1 regulates microglial homeostasis by deubiquitinating MYH9 to promote the pathogenesis of Alzheimer's disease

Jinfeng Sun[a,b,c,†], Fan Chen[b,d,†], Lingyu She[a,c], Yuqing Zeng[b], Hao Tang[b], Bozhi Ye[a,e], Wenhua Zheng[f], Li Xiong[a,b], Liwei Li[a,b], Luyao Li[e], Qin Yu[b], Linjie Chen[b], Wei Wang[d], Guang Liang[a,b,e,*], Xia Zhao[a,b,*]

[a]*Department of Pharmacy and Institute of Inflammation, Zhejiang Provincial People's Hospital, Affiliated People's Hospital, Hangzhou Medical College, Hangzhou 310014, China*
[b]*Zhejiang TCM Key Laboratory of Pharmacology and Translational Research of Natural Products, School of Pharmacy, Hangzhou Medical College, Hangzhou 311399, China*
[c]*Key Laboratory of Natural Medicines of the Changbai Mountain, Ministry of Education, Yanbian University, Yanji 133002, China*
[d]*Affiliated Yongkang First People's Hospital, Hangzhou Medical College, Yongkang 321399, China*
[e]*Chemical Biology Research Center, School of Pharmaceutical Sciences, Wenzhou Medical University, Wenzhou 325035, China*
[f]*Center of Reproduction, Development and Aging and Institute of Translation Medicine, Faculty of Health Sciences, University of Macau, Taipa 999078, China*

Received 26 February 2024; received in revised form 8 June 2024; accepted 26 July 2024

KEY WORDS

Alzheimer's disease;
YOD1;
Myosin heavy chain 9;
Microglia;
Inflammation;
Cognitive dysfunction;

Abstract Alzheimer's disease (AD) is the major form of dementia in the elderly and is closely related to the toxic effects of microglia sustained activation. In AD, sustained microglial activation triggers impaired synaptic pruning, neuroinflammation, neurotoxicity, and cognitive deficits. Accumulating evidence has demonstrated that aberrant expression of deubiquitinating enzymes is associated with regulating microglia function. Here, we use RNA sequencing to identify a deubiquitinase YOD1 as a regulator of microglial function and AD pathology. Further study showed that YOD1 knockout significantly improved the migration, phagocytosis, and inflammatory response of microglia, thereby improving

*Corresponding authors.
E-mail addresses: xiazhao@hmc.edu.cn (Xia Zhao), wzmcliangguang@163.com (Guang Liang).
[†]These authors made equal contributions to this work.
Peer review under the responsibility of Chinese Pharmaceutical Association and Institute of Materia Medica, Chinese Academy of Medical Sciences.

https://doi.org/10.1016/j.apsb.2024.11.020

Neurotoxicity;
Synaptic function

the cognitive impairment of AD model mice. Through LC−MS/MS analysis combined with Co-IP, we found that Myosin heavy chain 9 (MYH9), a key regulator maintaining microglia homeostasis, is an interacting protein of YOD1. Mechanistically, YOD1 binds to MYH9 and maintains its stability by removing the K48 ubiquitin chain from MYH9, thereby mediating the microglia polarization signaling pathway to mediate microglia homeostasis. Taken together, our study reveals a specific role of microglial YOD1 in mediating microglia homeostasis and AD pathology, which provides a potential strategy for targeting microglia to treat AD.

1. Introduction

Alzheimer's disease (AD) is a progressive neurodegenerative disorder and closely related to the toxic effects of microglia activation. Microglia are the most important immune cells in the central nervous system (CNS) and play an important role in the development, homeostasis, and disease of the CNS[1,2]. In recent years, genome-wide association studies (GWAS) have identified more than 25 genes strongly associated with AD, many of them are associated with neuroinflammation or specifically expressed in microglia[3]. The latest report also suggests that the pathogenic capacity of AD inflammation caused by microglia may exceed the currently generally accepted hypothesis of Aβ and tau proteins[4]. Imbalances in microglial homeostasis promote the release of inflammatory factors and the deposition of amyloid plaques, thereby impairing neuronal function and adversely affecting AD development[5,6]. In addition, imbalanced microglia abnormally label and excessively phagocytose neurons, while inhibiting the synaptic degeneration process caused by microglial phagocytosis alleviates neuronal cell damage[7,8]. Therefore, targeting proteins that regulate microglial homeostasis is crucial in the early stages of AD and can serve as important potential therapeutic targets.

Ubiquitination is a covalently reversible post-translational modification that participates in almost all cellular life activities, including cell signal transduction, cell fate determination, inflammation, immunity, and other pathophysiological processes[9]. Generally, ubiquitinating modification regulates the degradation and functions of substrate proteins. Deubiquitination is catalyzed by deubiquitinase enzymes (DUBs), which mainly interact with ubiquitinated target proteins to cleave or remove the ubiquitin chain of the target protein, thereby reversing the degradation of the target protein[10]. In AD, a large number of studies have found that disease-related neurofibrillary tangles and amyloid deposition are regulated by E3 ubiquitin ligases and DUBs. For example, inhibiting the function of USP10 significantly alleviates Tau deposition and cognitive decline[11]. Knockout of the deubiquitinase USP25 can significantly reduce amyloid plaque deposition in the brain tissue of AD model mice, thereby reversing synaptic function and cognitive function[12,13]. In the brains of 5 × FAD transgenic AD model mice, the deficiency of the E3 ubiquitin ligase Peli1 led to a significant enhancement of Aβ clearance by microglia, thereby inhibiting the deposition of Aβ in the brain[14]. However, current research mainly focuses on the regulation of toxic protein degradation and neuronal cell function regulated by DUBs, while the DUB-involved mechanisms in regulating microglia homeostasis and inflammation in AD pathogenesis remain not fully understood.

Our study mainly focuses on the role and function of DUBs in microglia during AD pathology. To find the key DUBs that regulate microglial function, we stimulated microglia with 20 μmol/L Aβ_{42} for 24 h and then performed RNA sequencing. The RNA-seq analysis indicated the potential involvement of a DUB, YOD1, in Aβ_{42}-challenged microglia. YOD1 is a member of the ovarian tumor protease family in DUBs and has been implicated in the regulation of ubiquitination in various diseases[15,16]. For example, YOD1 inhibits the progression of head and neck squamous cell carcinoma by inhibiting the ubiquitination and degradation of TRIM33[17]. YOD1 has been reported to be involved in the ER stress response induced by the mislocalization of unfolded proteins in mammalian cells[18]. In addition, YOD1 is associated with depression by regulating the IL-1 signaling pathway triggered by TRAF6/P62[19]. However, it is currently unclear whether YOD1 is involved in AD pathology.

The present study aimed to evaluate the role of YOD1 in AD and then explore the underlying molecular mechanism. In the present study, we showed that the deficiency of YOD1 inhibited the migration and phagocytosis of inflammatory microglia and promoted the transformation of microglia into M2 type. Mechanistically, we found that YOD1 may target MYH9, a key protein that maintains cell morphology, polarization, and phagocytosis, to regulate microglial function. The results of this study highlight the promise of YOD1 as a microglia-targeted therapy for AD.

2. Materials and methods

2.1. General reagents

Aβ_{42} (NH_2−DAEFRHDSGYEVHHQKLVFFAEDVGSNKGAII GLMVGGVVIA−COOH) was purchased from Ontores Biotechnologies (Zhejiang, China). JC-1 assay Kit (C2006), ROS assay Kit (S0033S), RIPA lysis buffer (P0013B), and MTT (ST316) were ordered from Beyotime Institute of Biotechnology (Shanghai, China). FITC-Aβ_{42} was obtained from GL Biochem (D8150, Shanghai, China). Penicillin/Streptomycin and Opti-MEM were ordered from Gibco (Carlsbad, CA, USA). Dimethyl sulfoxide (DMSO), Dulbecco's modified Eagle's medium (DMEM), and BSA (10711454001) were procured from Sigma (St. Louis, MO, USA). Annexin V-FITC/PI Apoptosis Detection Kit (556570) was obtained from BD Biosciences (San Diego, CA,

USA). Western Blot Marker (C520010) was bought from Sangon Biotech (Shanghai, China), and ECL Enhanced Chemiluminescent (P10300) was ordered from NCM Biotech (Suzhou, China). PVDF membrane (1620177) was bought from Bio-Rad. The antibodies used in this study are shown in Supporting Information Table S1. The primers used in this study are summarized in Supporting Information Table S2. A summary of AAV Vectors used in this study is listed in Supporting Information Table S3. The sources of RNA-seq analysis software are summarized in Supporting Information Table S4.

2.2. Experimental mice and treatment

Two AD models were used in this study: the acute pathological model induced by Aβ_{42} infusion in YOD1 knockout mice and the chronic pathological model was constructed by AAV injection in 3 × Tg (APP Swedish, MAPT P301L and PSEN1 M146V) mice. YOD1$^{-/-}$ mice on a C57BL/6 background, C57BL/6 WT mice, APP/PS1 mice, and 3 × Tg mice were obtained from Shanghai Biomodel Organism Science & Technology Development Co., Ltd. (Shanghai, China). Mice were housed in a pathogen-free room under the following housing conditions: 22 ± 2 °C, 50%−60% humidity, 12-h dark and 12-h light cycle, and fed a standard rodent diet in Hangzhou Medical College Animal Research Center. All animals received humane care according to the National Institutes of Health (USA) guidelines. The experimental protocol was approved by the Hangzhou Medical College Animal Ethics Committee (2023-052).

2.2.1. Aβ-infused YOD1 knockout mouse model

YOD1$^{-/-}$ mice and WT mice (8 weeks, 22−24 g) were randomly divided into four groups (n = 10 for each group): WT + sham, Aβ (Aβ_{42}-infused WT mice), YOD1$^{-/-}$ + sham, and YOD1$^{-/-}$ + Aβ_{42} (Aβ_{42}-infused YOD1$^{-/-}$ mice). For the stereotaxic brain injection operation, mice were anesthetized by intraperitoneal injection of 1% pentobarbital (40 mg/kg), and the mice's head hair was shaved after anesthesia. The mouse was fixed on the stereotaxic apparatus, and the head skin was cut with scissors to expose the anterior and posterior fontanelles. Place the microsyringe needle at bregma and return the coordinates to zero. Injection coordinates of the hippocampal CA1 region were determined based on the Paxinos and Franklin atlas (−2.0 mm posterior to bregma, ±1.5 mm lateral to midline, 1.5 mm deep from the dura). Subsequently, 5 μg/μL aggregated form of Aβ_{42} (incubated at 37 °C for 7 days) was injected into the CA1 area of the hippocampus on both sides of the mice. After injection, leave the needle in place for another 5 min and slowly withdraw the syringe needle. Sham surgery was performed on WT mice by injecting equal amounts of solvent.

2.2.2. AAV-injected 3 × Tg AD model

3 × Tg mice are currently the transgenic animal model closest to the pathological characteristics of AD. The mice gradually developed AD clinical pathological manifestations such as Aβ deposition, SP, and NFTS, as well as synaptic loss and neuronal degeneration in the cortex and hippocampus. To study YOD1 in AD microglia more specifically, we commissioned BrainVTA (Wuhan, China) to construct AAV vectors that specifically knockout YOD1 in microglia (YOD1-AAV): (rAAV-CX3CR1-DIO-mCherry-5′miR30-shRNA (YOD1)-3′miR30-WPREs) and microglial Cre AAV (rAAV-CX3CR1-CRE-WPRE-hGH pA). Then, two AAVs were mixed at a 1:1 ratio and injected into the hippocampus of 3 × Tg AD model mice using a brain stereotaxic injector. Behavioral testing was performed four weeks after the virus injection.

2.3. Behavioral tests

Similar to the previously described[20], the water maze test (MWM) and novel object recognition (NOR) were performed to evaluate the cognitive functions of mice in each group. Data collection and quantitative analysis for all behavioral tests were performed using an image automatic monitoring and processing system (VisuTrack, Shanghai, China). Briefly, for MWM, the mice were transferred to water containing a hidden platform. The time required for the mice to find the platform was recorded and the maximum time was limited to 60 s. Next, the platform was removed from the water maze and the mice were allowed to swim freely for 60 s to conduct a space exploration experiment. The number of times the mice crossed the platform and the time spent exploring the target quadrant were recorded. For NOR, mice were placed in an experimental device with two identical objects A, and the contact between the mice and the two objects was recorded for 5 min. After 24 h, one of the A objects was replaced with the B object and it was recorded with a video device for 5 min. The cognitive index (recognition index, RI) was calculated as Eq. (1):

$$\text{RI}\ (\%) = \text{New object}/(\text{New object} + \text{Old object}) \times 100 \quad (1)$$

2.4. Cell culture and transfection

NIH/3T3 cells (GNM 6) were purchased from the Shanghai Institute of Biochemistry and Cell Biology (Shanghai, China). BV2 cells (SNL-155) were purchased from Wuhan Shangen Biotechnology Co., Ltd. (Wuhan, China). BV2 cells and NIH/3T3 cells were cultured in DMEM (Gibco) supplemented with 10% FBS and 1% antibiotics (100 μg/mL streptomycin, 100 U/mL penicillin). The cells were cultured at 37 °C and 5% CO_2.

YOD1 and MYH9 in BV2 cells were silenced using siRNAs and the siRNA sequences for mouse YOD1 and MYH9 were designed by Genepharma (Shanghai, China). Negative control transfections included scrambled siRNA sequences. Cells were transfected with siRNA using Lipofectamine 2000 (168019, Thermo Fisher Scientific) according to the manufacturer's protocol. Flag-YOD1, Flag-YOD1-C155A, Flag-YOD1-CH262A, Flag-YOD1-H337A, YOD1 mut1 (no UBX-like domain), YOD1 mut2 (no otubain domain), YOD1 mut3 (no C2H2-type domain), His-MYH9, HA-Ub, HA-K48 and HA-K63 were obtained from Tsingke Biotechnology Co., Ltd. These plasmids were transfected to cells using the Lipofectamine 8000 Transfection Reagent (C0533FT, Beyotime Biotechnology).

2.5. Golgi staining

After the mice were deeply anesthetized, the hippocampus of the mouse brain tissue was dissected, followed by Golgi staining using the FD Fast Golgi Staining Kit according to the manufacturer's protocol. The brain tissue was gently immersed in Golgi stain mixed with equal volumes of solutions A and B in the dark at

room temperature. After 48 h of soaking, fresh Golgi stain was added to the samples and incubated for an additional 14 days at room temperature in the dark according to the manufacturer's instructions. Next, the tissue was transferred to solution C and incubated in the dark at room temperature for 7 days. The tissue block was removed, the tissue was cut into 100−200 μm thick slices using a freezing microtome at −20 to −22 °C, and stained with staining solution for 10 min at room temperature in the dark. The slides were mounted on glycerol gelatin, and images of dendritic spines were obtained using confocal laser microscopy (HD25, Japan).

2.6. *Immunocytochemistry (ICC)*

Appropriately treated BV2 cells were fixed with 4% paraformaldehyde for 15 min and then permeabilized with 0.3% Triton X-100 in PBS for 20 min at room temperature. Cells were then blocked with 1% BSA for 1 h and incubated with primary antibodies (1:100) overnight at 4 °C. The next day, cells were washed three times with 1 × PBS and then incubated with Alexa Fluor 488 or Alexa Fluor 594 secondary antibodies (1:500; Cell Signaling Technology) for 2 h at room temperature. The nuclei were counterstained with DAPI (P0131, Beyotime). Images of the staining were acquired using a Nikon A1 confocal microscope (HD25).

2.7. *Immunofluorescence (IF)*

For IF staining of mouse brain sections, mice were deeply anesthetized and transcardially perfused with 1 × PBS. After the brain tissue was fixed in 4% PFA for about 24 h, it was dehydrated using gradients of 20% sucrose and 30% sucrose solutions. Then, the tissue was embedded in OCT and cut into 20 μm sections using a cryostat (Leica CM3050, Leica, Germany). Brain sections were permeabilized with 0.3% Triton X-100 in PBST buffer, followed by blocking with 10% BSA for 1 h at room temperature. The brain sections were incubated with the indicated primary antibodies overnight at 4 °C and then stained with secondary antibodies. Nuclei were counterstained with DAPI (Sigma, D6578), and the images of the staining were acquired using a Nikon A1 confocal microscope (HD25).

2.8. *RNA isolation and quantitative real-time PCR*

Total RNA was isolated from cultured cells and brain tissues using TRIZOL Reagent (Thermo Fisher, 15596026) according to the manufacturer's instructions. For RT-PCR analysis, cDNA was generated with a PrimeScript RT reagent Kit (Takara, RR037A). Real-time PCR was subsequently conducted using TB Green Premix Ex Taq II (Takara; RR820A) on CFX96 Touch Real-Time PCR Detection System (CFX96, Bio-Rad, Singapore). Relative expression was calculated by the $2^{\Delta\Delta Ct}$ method with GAPDH normalization. Primers for genes were obtained from Thermo Fisher.

2.9. *Liquid chromatography-tandem mass spectrometry (LC−MS/MS)*

293T cells were transfected with Flag-YOD1- or Flag-NC and proteins were harvested 24 h later. Protein use RIPA lysis buffer to extract cellular proteins supplemented with protease inhibitors. Use Flag-tagged affinity magnetic beads for immunoprecipitation. The immunoprecipitates were washed three times with PBST Buffer and separated by SDS-PAGE. Gels were excised separately from the Flag-YOD1- or Flag-NC group. The excised gel samples were analyzed by LC−MS/MS at Hangzhou Jingjie Biotechnology Co., Ltd. (Hangzhou, China).

2.10. *Transwell migration assay*

To evaluate the effect of YOD1 on microglial migration, a Transwell assay was performed using 8-μm-pore-diameter inserts (14241, Labselect, China). Briefly, 1×10^5 BV2 cells were plated in the upper chamber with 500 μL of blank medium (FBS-free DMEM medium), and the chamber was then placed within the bottom wells (12-well plate) containing 1.5 mL of 10% FBS medium, followed by incubation for 24 h. The BV2 cells on the upper membrane were removed with a cotton swab, and the cells on the lower surface of the membrane were fixed with 100% methanol for 20 min. Then the cells were stained with crystal violet for 20 min at room temperature. Images were acquired through crossed polarizers under a Leica microscope (DMi8, Germany), and the number of migrating cells was manually quantified.

2.11. *Microglia phagocytosis assay*

BV2 cells were seeded on coverslips in 12-well plates at a density of 1×10^4 cells/well and cultured in an incubator with 5% CO_2 at 37 °C. After attaching, cells were transfected with Yod-1 interference plasmid or control plasmid with liposome 2000 for 24 h. Then incubated with/without FITC-Aβ_{42} peptides in DMEM to reach a final concentration of 20 μmol/L for 2 h. After incubation, the medium containing FITC-Aβ was removed, and the cells were washed three times with 1 × PBS. BV2 cells were collected by centrifugation at 1000 rpm for 5 min and resuspended in ice-cold 1 × PBS solution. The phagocytosed Aβ content in BV2 cells was analyzed by flow cytometry, and PBS solution (pH 4.4) was added to the sample for 1 min incubation before flow cytometry analysis to quench the cell surface-bound Aβ. In addition, we performed IF observation of Aβ phagocytosis by microglia, and the cells treated similarly as above were fixed with 4% PFA for 15 min. Observe and analyze the amount of green fluorescence inside microglia using a Nikon A1 confocal microscope.

2.12. *Co-immunoprecipitation (Co-IP)*

Proteins from transfected cells or brain tissues and cells were lysed on ice using RIPA buffer (P0013B; Beyotime Biological Technology, Shanghai, China) supplemented with protease inhibitor cocktail (P1045, Beyotime). Half the volume of the supernatant is retained as input, the remaining was incubated with antibodies overnight at 4 °C, followed by the addition of protein A/G beads for 2 h at room temperature. The immunocomplexes were then washed with 500 μL of lysis buffer 3 times and analyzed by Western blotting. Briefly, the protein concentration of cells/tissue samples was assessed using a BCA protein assay kit according to the manufacturer's instructions.

2.13. *Western blotting*

Samples with the same concentration of proteins were separated by 10% SDS-PAGE gels and later transferred to the PVDF

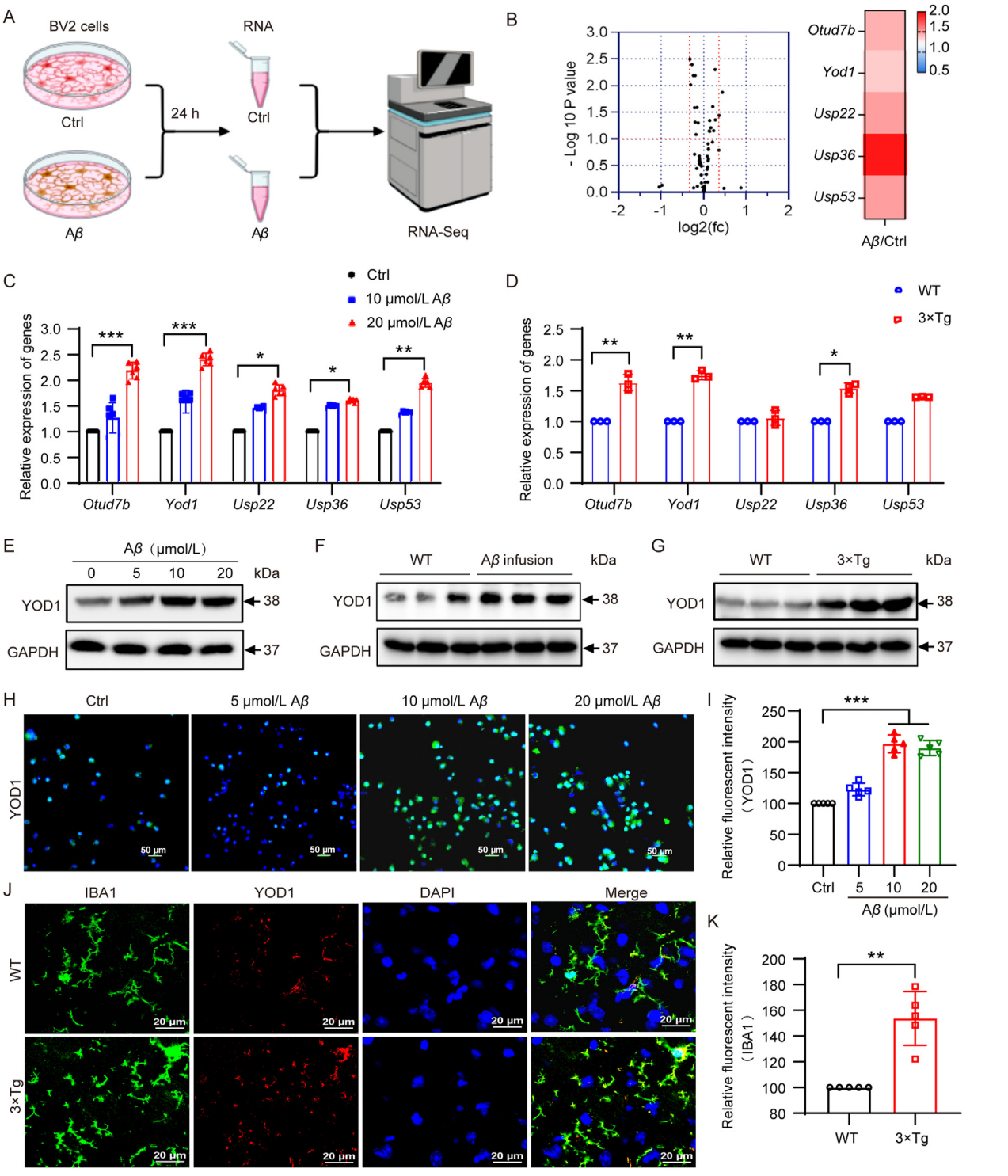

Figure 1 YOD1 was up-regulated in the brains of AD models. (A) RNA-seq analysis of BV2 cells treated with Aβ for 24 h (n = 3 mice/group). (B) Bioinformatics analysis of DUBs (deubiquitinating enzymes) in RNA-seq. Among them, the expression of *Otud7b*, *Yod1*, *Usp22*, *Usp36* and *Usp53* increased significantly compared with the control group. (C) qPCR analysis of *Otud7b*, *Yod1*, *Usp22*, *Usp36* and *Usp53* mRNA expression in Aβ induced BV2 cells. (D) qPCR analysis of *Otud7b*, *Yod1*, *Usp22*, *Usp36*, and *Usp53* mRNA expression in 3 × Tg AD models (n = 6 samples/group for C and D panels). (E) Western blot analysis of YOD1 in Aβ induced BV2 cells. (F) Western blot analysis of YOD1 in Aβ infusion model mice. (G) Western blot analysis of YOD1 in 3 × Tg AD model mice. (H, I) ICC analysis of YOD1 in Aβ induced BV2 cells (n = 5 images/group). (J, K) IF analysis of YOD1 in 3 × Tg AD model mice. Data are mean ± SEM; *$P < 0.05$, **$P < 0.01$, ***$P < 0.001$.

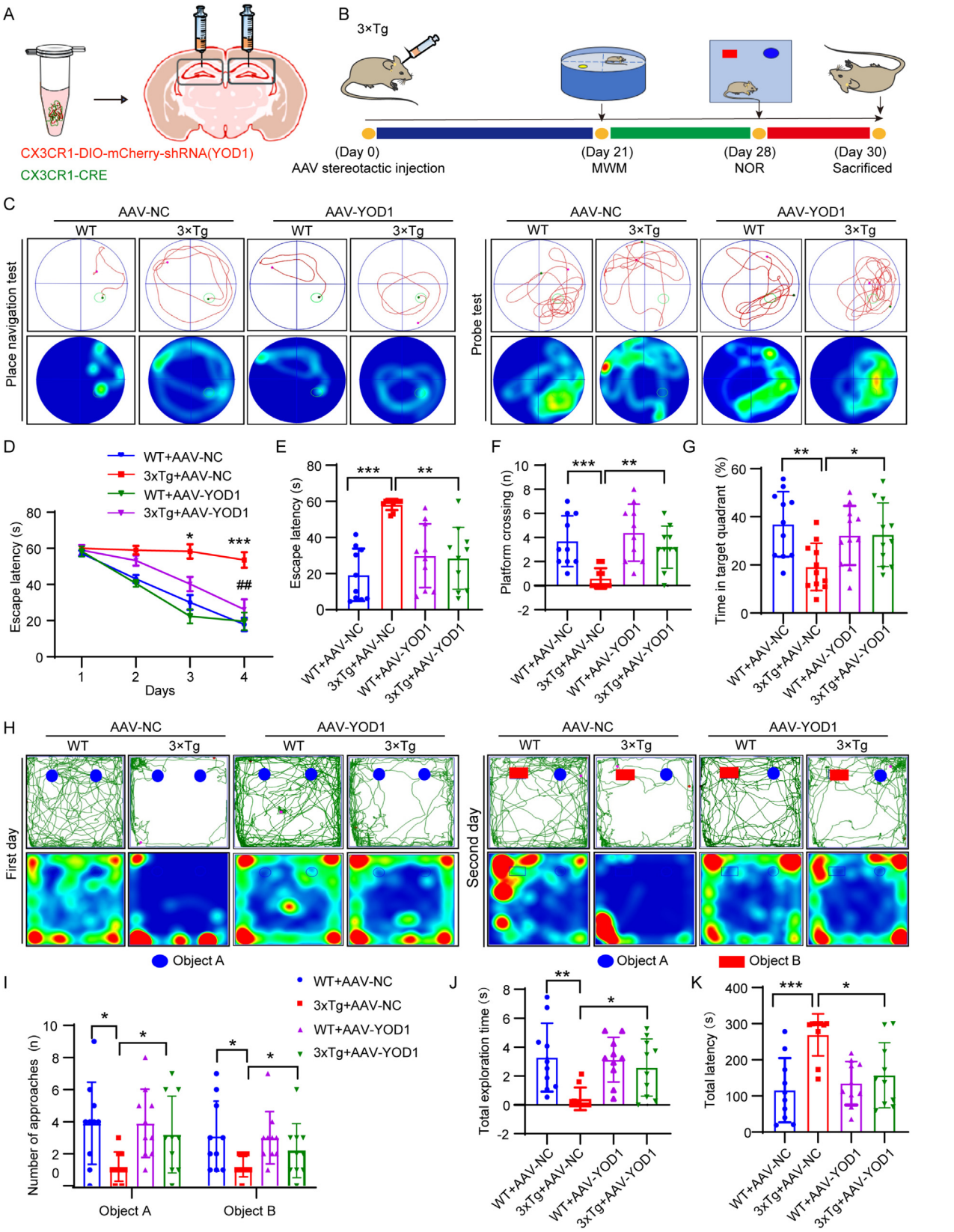

Figure 2 Hippocampal injection of microglial AAV-YOD1 improved cognitive deficits in 3 × Tg mice. (A) Schematic diagram of AAV virus injection into the hippocampus. (B) Behavioral experimental procedures and time points after AAV-YOD1 injection. (C) Representative trajectory curve of place navigation test and spatial probe test. (D, E) Time required for mice to find the platform hidden under the water in the Place navigation test (Escape latency). (F) The average number of times mice in each group crossed the platform within 60 s after removing the platform. (G) Time spent in the target quadrant where the platform is located after the platform is removed. (H) Representative images of novel

membrane at 260 mA for 90 min. The PVDF membranes containing protein bands were blocked with 3% BSA for 1 h at room temperature, and the membranes were incubated with selective primary antibodies overnight at 4 °C. In the following day, horseradish peroxidase (HRP)-conjugated secondary antibody was incubated for another 2 h at room temperature. The specific protein bands were analyzed using the Bio-Rad Gel Doc XR documentation system (Chemidoc MP, Bio-Rad, Singaporean) and quantified using Image J software.

2.14. Statistical analysis

All the data are presented as mean ± standard error of mean (SEM). Each experiment was carried out in triplicates. For the MWM test, escape latency times in the hidden platform trial were analyzed *via* two-way ANOVA of repeated measures. Statistical differences were analyzed by one-way ANOVA in combination with *post hoc* Tukey's test ($\alpha = 0.05$) to assess the difference between any two groups by using GraphPad Prism 8.0 statistical software (GraphPad Software, Inc., San Diego, CA, USA).

3. Results

3.1. YOD1 is up-regulated in Aβ-induced microglia and AD model mice

By conducting RNA sequencing analysis of Aβ-induced microglia (Fig. 1A), we observed abnormal expressions of DUB genes in microglia stimulated by Aβ. Among them, *Otud7b*, *Yod1*, *Usp22*, *Usp36*, and *Usp53* are the top five genes with significant overexpression levels compared with the control group (Fig. 1B). Next, we used qPCR to detect the expression of these five genes in Aβ-induced microglia and 3 × Tg mice. The results find that compared with the control group, the expression of *Yod1* was the most significant (Fig. 1C and D). Next, we treated BV2 cells with different concentrations of Aβ (5−20 μmol/L) and tested the expression changes of YOD1. Western blot results show that the expression of YOD1 was increased in a dose-dependent manner in BV2 cells after Aβ treatment (Fig. 1E). To further confirm that YOD1 is involved in the pathology of AD, we selected hippocampus brain tissues of different AD model mice for Western blot analysis. Results show that the protein level of YOD1 was significantly increased in Aβ infusion model mice (Fig. 1F) and 3 × Tg model mice (Fig. 1G). The effect of YOD1 in BV2 cells and brain tissue sections was further analyzed by immunofluorescence staining, and the results show that YOD1 was highly expressed in Aβ-induced BV2 cells (Fig. 1H and I) and 3 × Tg model mice (Fig. 1J and K). The above results suggest that microglia YOD1 was up-regulated in the brains of AD models.

3.2. Microglial YOD1 deficiency alleviates cognitive impairment in 3 × Tg mice

To determine the role of YOD1 in AD, AAV targeting microglia-specific YOD1 knockout (AAV-YOD1) was injected into the hippocampus of age- and sex-matched wild-type (WT) and 3 × Tg mice (Fig. 2A). Here, we injected AAV into the mouse hippocampus at two points to ensure that the injected virus covered the whole hippocampus. As expected, the fluorescence imaging system detected that AAV could completely cover the hippocampus and be successfully expressed (Supporting Information Fig. S1A). Furthermore, we double-stained the YOD1 with microglia marker IBA1 and found that YOD1 in microglia was successfully knocked down (Fig. S1B). Three weeks after injection, Morris water maze (MWM) and novel object recognition assay (NOR) were performed to assess learning and memory abilities (Fig. 2B). The movement trajectories of each group of mice in the MWM test (Fig. 2C) shows that the average escape latency of microglia YOD1 knockdown mice was significantly lower than that of 3 × Tg mice (Fig. 2D and E). After removing the platform, mice in the YOD1 knockout group crossed the platform more times and stayed in the target quadrant longer than mice in the 3 × Tg model (Fig. 2F and G). We further validated our results using the NOR test (Fig. 2H). Results show that compared with the 3 × Tg group, the YOD1 knockout group mice increased the number of times to explore new object (Fig. 2I), the total latency to touch novel object was reduced (Fig. 2J) and the time they spent exploring new object increased (Fig. 2K). These data demonstrate that knockdown of microglia YOD1 significantly improves cognitive impairment in 3 × Tg model mice.

3.3. Microglial YOD1 deficiency improves microglial function and neuron damage in 3 × Tg mice

Excessive activation of microglia leads to an imbalance in their homeostasis and produces a large amount of cytotoxic molecules[21]. To further investigate the impact of YOD1 on microglial activation, we analyzed the expression levels of IBA1 (microglial marker) in the hippocampus of different groups of mice. Results show that YOD1 knockdown significantly reduced the number of IBA1-positive cells, indicating that YOD1 knockdown significantly inhibited microglial activation (Fig. 3A and B). Microglia have the function of synaptic remodeling, and learning and memory functions are highly dependent on synaptic plasticity. We next examined synaptic plasticity. IF staining of mouse hippocampus showed that the number of cells expressing neurite cytoskeletal microtubule-associated protein 2 (MAP2) in the YOD1 knockout group was significantly increased compared with the 3 × Tg group (Fig. 3C and D). Excessive activation of microglia causes damage to neuronal cells. Then, we used Golgi staining to visualize synaptic spines and found that the number of synaptic spines in microglia in 3 × Tg mice was significantly increased after YOD1 knockout (Fig. 3G and H). We further detected the effect of YOD1 knockdown on neuronal cell apoptosis in animal models through IF staining and results show that microglia YOD1 knockout reduced the loss of positive NeuN + neurons in 3 × Tg mice (Fig. 3E and F). The regulating actions of YOD1 on neuronal cell loss may result from two possible mechanisms: A) YOD1 deletion mediates Aβ induced neuronal cell damage and B) YOD1 deletion reduces neuronal cell damage by acting on microglia. To preliminary verify the role of YOD1 in neuronal cells, we knocked down YOD1 in PC12 cells

object recognition test. (I) A total number of object approaches was explored on the 2nd day. (J) Total time to explore new object B. (K) Total latency of new object approaches. Data are mean ± SEM, $n = 10$ mice/group for C−K panels; $^{*}P < 0.05$, $^{**}P < 0.01$, $^{***}P < 0.001$.

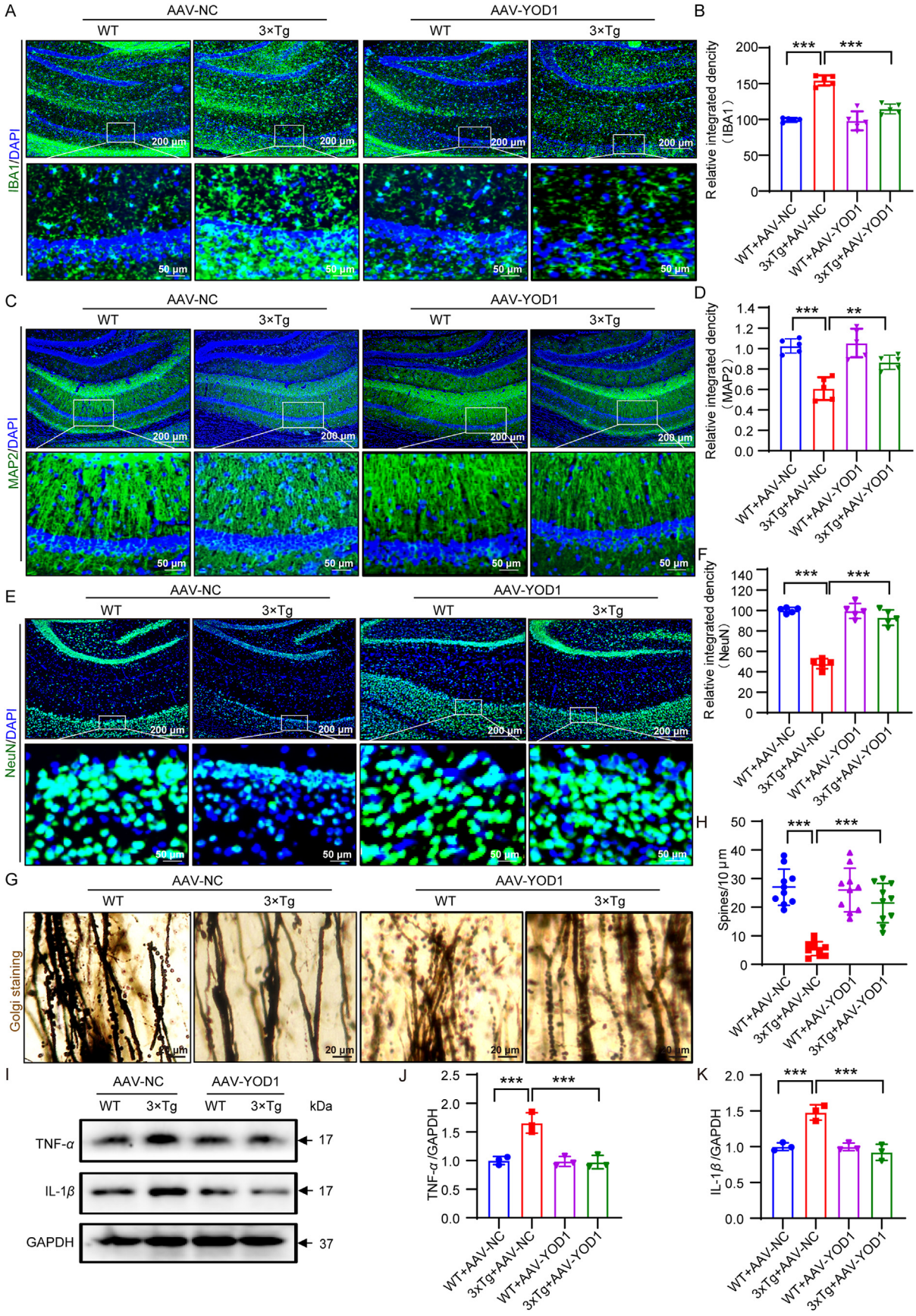

Figure 3 Microglia YOD1 deficiency improves synaptic plasticity, microglial activation and neuron apoptosis in 3 × Tg mice. (A) IF staining detects microglial activation (IBA1) in the hippocampus of mice. (B) Fluorescence quantification of IBA1 staining in panel A. (C) IF staining

and then treated with Aβ for 24 h. MTT results showed that YOD1 knockdown did not significantly improve the cell viability of PC12 cells (Supporting Information Fig. S2). To verify whether microglia YOD1 can directly affect neuronal cell apoptosis, we collected the microglia culture medium after YOD1 knockdown and then used it to culture neuronal cells. Results show that YOD1 can regulate neuronal apoptosis by acting on microglia (Supporting Information Fig. S3). Therefore, we believe that YOD1 in microglia participates in mediating the apoptosis of neuronal cells. To confirm the effect of YOD1 on the expression of inflammatory factors, we used Western blot to test the expression of TNF-α and IL-1β in the hippocampus of mice. Results show that YOD1 knockdown inhibited the expression of TNF-α and IL-1β in 3 × Tg mice (Fig. 3I−K). These results indicate that YOD1 is associated with microglial function and neuron damage.

3.4. *YOD1 regulate cognitive impairment in Aβ infusion YOD1$^{-/-}$ mice*

In order to further explore the role and mechanism of YOD1 in AD, we commissioned Shanghai Southern Model Biology Company to construct YOD1 knockout (YOD1$^{-/-}$) mice (Supporting Information Fig. S4A and S4B). After purification, we identified positive mice by qPCR and Western blot (Fig. S4C and S4D), and used brain stereotaxic $A\beta_{42}$ (10 μg/mouse) was injected into the hippocampus of mice to induce an acute model of microglia activation and nerve cell damage, and the WT mice were infused with the same amount of solvent. Behavioral testing was conducted two weeks after modeling (Fig. 4A). The movement trajectories of mice in each group in the MWM test are shown in Fig. 4B and C. Compared with the WT group, the average escape latency of mice injected with Aβ was significantly increased, while the average escape latency was significantly decreased after YOD1 was knocked out (Fig. 4D and E). Consistent with the results in 3 × Tg mice, after removing the platform, mice in the YOD1$^{-/-}$ group stayed in the target quadrant longer (Fig. 4F) and crossed the platform more times than Aβ infusion model mice (Fig. 4G). To further verify the effect of YOD1 on cognitive impairment, we performed the NOR test. The movement trajectories of mice in each group of mice in the NOR test are shown in Fig. 4H and I. Compared with the WT group, the total number of approaches to object A on the first day was significantly increased in the YOD1 knockout group (Fig. 4J). On the second day, we replaced one of the old objects A with a new object B and found that the total approach and total latency of the new object B (Fig. 4K and L) in the YOD1$^{-/-}$ group was significantly increased compared with the Aβ infusion model group. These data demonstrate that knockdown of YOD1 significantly improves cognitive impairment in Aβ infusion model mice.

3.5. *YOD1 regulate AD-type pathology in Aβ infusion YOD1$^{-/-}$ mice*

To further evaluate the effect of YOD1 knockout on the pathology of Aβ infusion model mice, we used IF and Golgi staining to detect changes in microglia activation, synaptic plasticity, and neuronal damage. Results showed that the number of microglia was increased in Aβ-infused mice, while YOD1 knockout significantly reduced the number of activated microglia cells (Fig. 5A and B). We further examined the apoptosis of neuronal cells. We found that YOD1 knockout reversed the Aβ-induced decrease in the number of Neut-positive cells (Fig. 5A and C). Similarly, Golgi staining results showed that YOD1 knockout reversed the synaptic spine loss caused by Aβ infusion (Fig. 5A and D). Western blotting further verified that YOD1 knockout significantly increased the protein level of MAP2 and postsynaptic density protein 95 (PSD95) in AD model mice (Fig. 5E−G). In addition, compared with the Aβ infusion group, YOD1$^{-/-}$Aβ mice reduced the expression of TNF-α and IL-1β (Fig. 5H−J). Together, these results indicated that YOD1 deficiency improves AD-type pathology in Aβ infusion model mice.

3.6. *YOD1 deficiency inhibits microglial migration, phagocyte function and inflammatory response*

We examined the effect of YOD1 silencing on inflammation in microglia. First, we screened the optimal conditions for YOD1 silencing in microglia (Fig. 6A). Next, Aβ was added to YOD1-silenced microglia to induce inflammation, and samples were collected for qPCR to detect the expression of inflammatory factors. Obtain results showed that Aβ caused a significant increase in M1-type pro-inflammatory factors and a significant decrease in M2-type anti-inflammatory factors in microglia, a phenomenon that could be improved by silencing YOD1 (Fig. 6B and C).

As the most important immune cells in the brain, microglia modify neurons through phagocytosis and participate in the regulation of neuronal regeneration and synaptic pruning[22,23]. So, we explored the effect of YOD1 on microglial phagocytosis. Cells over-expressing or silencing YOD1 were treated with Aβ for 24 h, and flow cytometry was used to detect the role of YOD1 in regulating microglial phagocytosis. We found that the phagocytic function of YOD1-silenced microglia was significantly improved, while the phagocytosis of microglia was reduced after YOD1 was over-expressed (Fig. 6D). To further verify our results, we constructed FITC-Aβ to replace Aβ in the treatment of microglia. The obtained results show that the fluorescence in microglia was significantly higher after YOD1 was silenced than in the FITC-Aβ group, while the fluorescence intensity decreased after YOD1 was over-expressed (Fig. 6E and F). The above results suggest that YOD1 can regulate the phagocytosis function of microglia.

Over-activated microglia amplify inflammatory responses and neuronal damage due to migration[24,25]. Wound scratch test results show that YOD1 silencing inhibited Aβ-induced microglial migration, whereas overexpression of YOD1 promoted migration. Similarly, the *trans*-well assay shows that YOD1 silencing reduced microglial migration, which further confirmed the results of the wound scratch assay (Fig. 6G−I). Taken together, these findings confirm that YOD1 can participate in the regulation of microglial function.

detects synaptic plasticity (MAP2) indicators in the hippocampus of mice. (D) Fluorescence quantification of MAP2 staining in panel A. (E) IF staining detects neuronal cell (NeuN) apoptosis in the hippocampus of mouse. (F) Fluorescence quantification of NeuN staining in panel A ($n = 5$ images/group for A−F panels). (G) Golgi staining visualizing synaptic spines. (H) Analysis of synaptic spine density. (I) Western blot detects the expression of inflammatory factors TNF-α and IL-1β in brain tissue ($n = 3$ samples/group). (J, K) Quantification of TNF-α and IL-1β in panel G, respectively. Data are mean ± SEM; $^{**}P < 0.01$, $^{***}P < 0.001$.

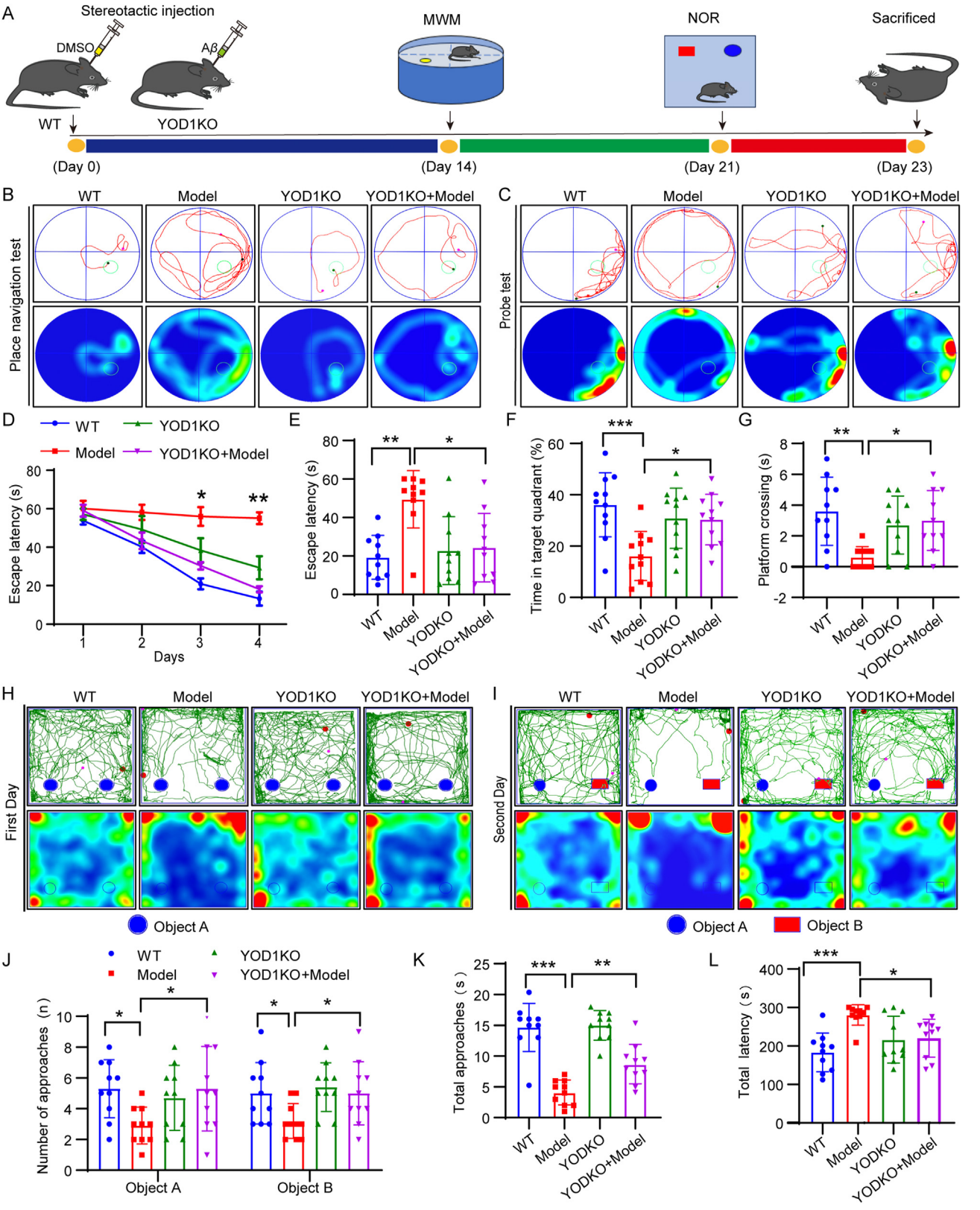

Figure 4 YOD1 knockout improves cognitive impairment in Aβ infusion model mice. (A) Injection of Aβ into the hippocampus of YOD1 knockout mice and subsequent experimental procedures. (B) Representative trajectory curve of place navigation in the first four days. (C) Representative trajectory curve of the spatial probe after removing the hidden platform on Day 5. (D, E) Time required to find the hidden platform (escape latency). (F) Percentage of time mice spent in the target quadrant during the spatial probe test. (G) Number of times mice crossed the hidden platform in the Spatial probe test. (H) Exploring the trajectories of two identical objects A on the first day. (I) Explore the trajectory of old and new objects on the 2nd day. (J) Total number of new object approaches was explored. (K) Time to explore new object. (L) The total latency of new object approaches was explored. Data are mean ± SEM, $n = 10$ mice/group for B−L panels; $^{*}P < 0.05$, $^{**}P < 0.01$, $^{***}P < 0.001$.

3.7. *MYH9 is a potential substrate of YOD1*

DUBs exert their biological functions by affecting the degradation or function of substrate proteins[26,27]. To determine the substrate proteins regulated by YOD1 in microglia, we transfected NIH/3T3 cells with empty Flag vector or Flag-YOD1 vector and performed immunoprecipitation assay combined with liquid chromatography-tandem mass spectrometry (LC−MS/MS) method to analyze potential substrate proteins of YOD1 (Fig. 7A). To discover the proteins that YOD1 may bind to, we performed relative quantification of the two groups of proteins in the mass spectrometry and obtained the top ten proteins with high YOD1-binding affinity: MYH9, RPLP2, EEFLA1, ACTB, HSP90AB1, HSPA1B, MYL6, TPM3, TUBA1B, PKM (Supporting Information Fig. S5). Among potential YOD1-binding proteins, MYH9 is highly associated with microglial function in AD, and its role matches the effect of YOD1 in AD. MYH9 is a member of the myosin II subfamily and plays an important regulatory role in maintaining cell morphology, polarization, and phagocytosis in key cellular processes[28,29]. Studies have found that inhibiting the expression of MYH9 can inhibit the activation of M1 pro-inflammatory microglia and exert a neuroprotective effect[30,31]. In YOD1 mass spectrometry analysis, a total of 21 MYH9 peptides were detected, and the top five MYH9 secondary peptide maps are shown in Fig. S5B, and one representative specific peptide among them is shown in Fig. 7B. Next, we performed a preliminary verification of the mass spectrometry results and found that MYH9 co-localized with YOD1 through dual fluorescence staining (Fig. 7C). Further, Co-IP verification found that the interaction between YOD1 and MYH9 was significantly increased in brain tissue (Fig. 7D), microglia cells (Fig. 7E), and NIH/3T3 cells (Fig. 7F). Subsequently, we further explored which domain of YOD1 binds to MYH9.YOD1 has three domains: UBX-like domain (45-123aa), OTU domain (144-269aa), and C2H2 type domain (313-337aa). To determine the interaction domain between YOD1 and MYH9, we generated three YOD1 truncation mutants (Fig. 7G). By co-transfecting MYH9 and mutated YOD1 plasmids in NIH/3T3 cells, it was determined that when amino acids 313 to 317 are deleted, YOD1 failed to bind MYH9, while YOD1 with mutations in other domains can still bind to MYH9 and function (Fig. 7H).

3.8. *YOD1 regulates the deubiquitination of MYH9*

YOD1, as a deubiquitinase, can regulate substrate degradation and stability[32]. We then examined whether YOD1 could regulate MYH9 ubiquitination. To do this, we co-transfected HA-Ub, His-MYH9, and Flag-YOD1 plasmids in NIH/3T3 cells respectively. We then treated cells with MG132 to prevent proteasomal degradation of MYH9 protein. The results showed that YOD1 can reduce the ubiquitination of MYH9 (Fig. 7I). Next, we further explored the regulatory mechanism of MYH9 ubiquitination by YOD1. We co-transfected His-MYH9, Flag-YOD1 and mutant ubiquitin plasmids in NIH/3T3 cells respectively, retaining only the K48 and K63 active sites. We then treated cells with MG132 to prevent proteasomal degradation of MYH9 protein. We observed that the HA-UbK48 plasmid was sufficient to reduce the ubiquitination of MYH9 in the presence of YOD1, with levels that were significantly increased compared with WT HA-Ub (Fig. 7J). In NIH/3T3 cells, Co-IP was used to confirm that the central OTU region of MYH9 affects the ubiquitination of MYH9 by YOD1 (Fig. 7K). DUB can catalyze the hydrolysis of the amide bond between ubiquitin molecules and substrate proteins through active sites such as cysteine and histidine. Therefore, we mutated the three active sites of YOD1 (cysteine at position 155, histidine at position 262, and histidine at position 337) (Fig. 7G). We found that mutate YOD1 at H262A can no longer remove ubiquitin molecules from MYH9 (Fig. 7L). These results indicate that histidine at position H262 of YOD1 is involved in removing ubiquitin molecules from MYH9, thereby preventing its degradation.

3.9. *YOD1 regulates microglial function through deubiquitinating MYH9*

We first tested whether silencing or overexpression of YOD1 could regulate MYH9 expression in microglia. Western blot analysis found that Aβ treatment increased the protein expression of YOD1 and MYH9. After silencing YOD1, the expression of MYH9 was reduced (Fig. 8A); conversely, YOD1 overexpression increased the expression of MYH9 (Fig. 8B). The results were further confirmed in Aβ- infusion YOD1$^{-/-}$ model mice (Fig. 8C) and AAV-injected 3 × Tg model mice (Fig. 8D). These data indicate that YOD1 regulated MYH9 protein stability in microglia. To further confirm whether MYH9 mediates YOD1's regulation of microglial function. We co-transfected YOD1 overexpression and MYH9-silencing plasmids in microglia and evaluated the changes in microglial inflammation, migration, and phagocytosis. We confirmed that silencing MYH9 inhibited YOD1 overexpression-induced overexpression of inflammatory factors in microglia (Fig. 8E and F). In addition, silencing MYH9 also improved the phagocytosis function of microglia (Fig. 8G) and reduced microglial migration (Fig. 8H−J). Taken together, we speculate that YOD1 regulates microglial function in microglia through MYH9.

4. Discussion

In this study, we found that the expression of YOD1 was upregulated in microglia and AD model mice. Specific knockdown of microglia YOD1 significantly improves cognitive impairment and neuropathology in AD model mice. Using mass spectrometry combined with Co-IP analysis, MYH9 was identified as a key substrate of YOD1 in microglia. Mechanistically, YOD1 regulates K48-linked MYH9 deubiquitination through its active site H262, inhibiting the proteasomal degradation of MYH9, thereby enhancing MYH9 stability and protein levels to promote microglial inflammation and AD pathology. Our data support that targeting microglial YOD1 may be a potential treatment for AD.

During the pathogenesis of AD, microglia exert diversified functions, including migration, phagocytosis, and production of various cytokines and chemokines[33]. Multiple studies have shown that microglial dysfunction is closely related to the development of AD[4,34]. Overactivated microglia can mistakenly label normal neurons, causing synapses of normally functioning neurons to be engulfed by microglia, causing synaptic degeneration[35,36]. Activated microglia can lead to persistent inflammation, and the migration of inflammatory microglia further worsens the inflammatory environment in the brain and causes neuronal cell damage. A variety of DUBs have been explored to be involved in the

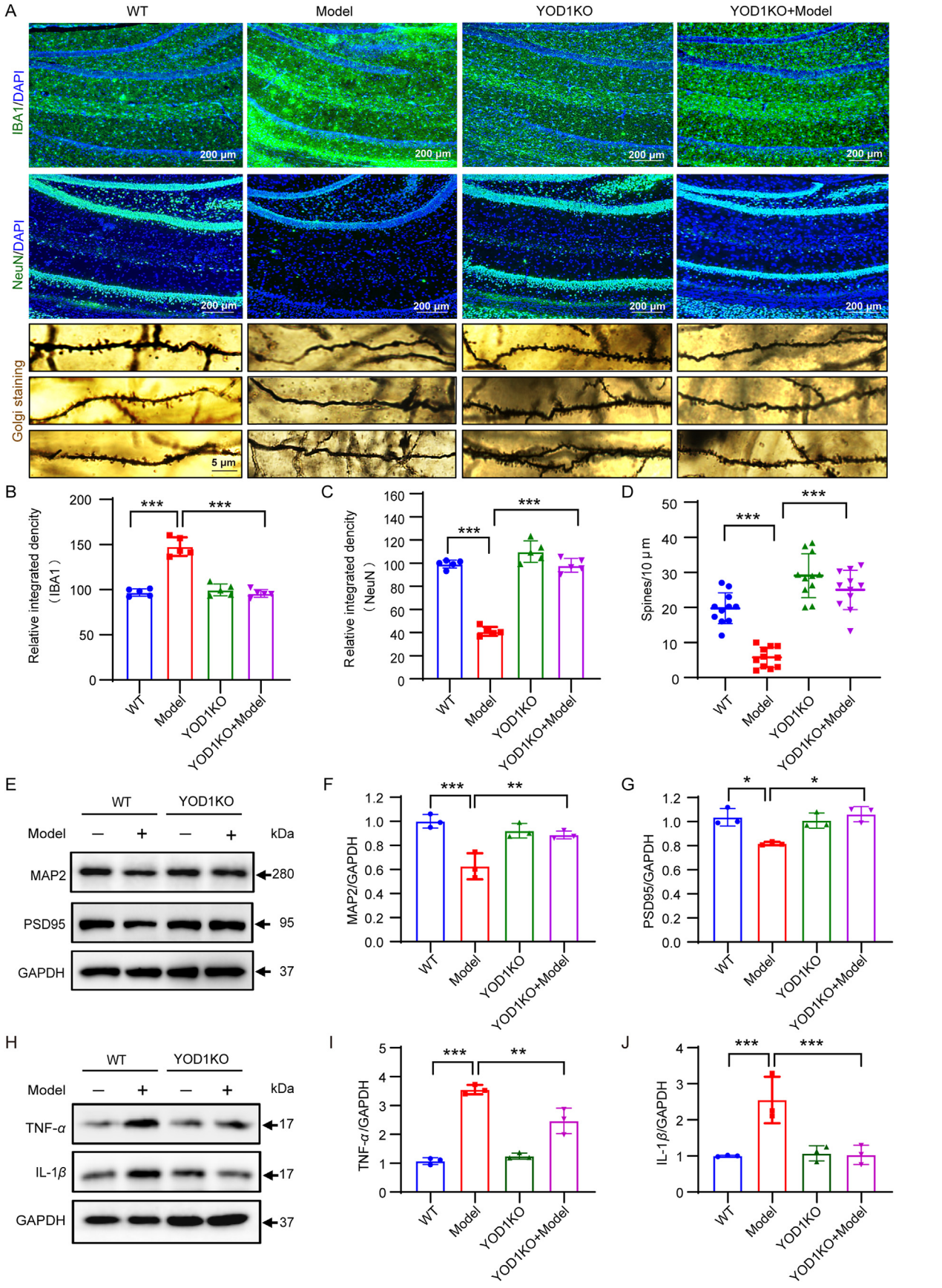

Figure 5 YOD1 deficiency improves AD-type pathology in Aβ infusion model mice. (A) Detection of microglial activation (IBA1) and neuronal cell (NeuN) apoptosis in brain tissue by IF staining. Golgi staining visualizing synaptic spines. (B) Fluorescence quantification of IBA1

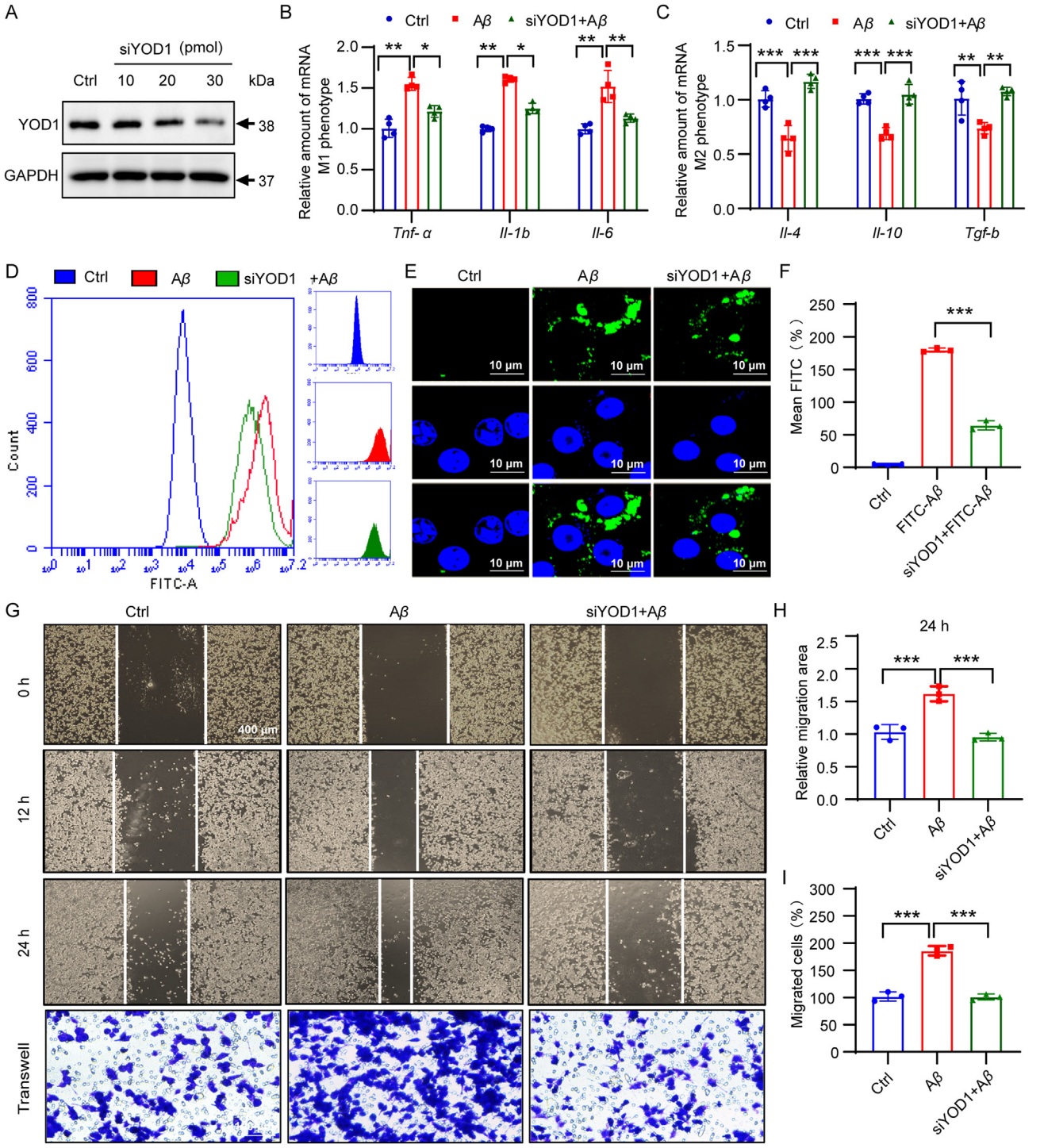

Figure 6 YOD1 deficiency inhibits microglial migration, phagocytic function and inflammatory response. (A) Western blot detects the silencing efficiency of YOD1 ($n = 3$ samples/group). (B) qPCR detection of the expression of M1-type pro-inflammatory factors. (C) qPCR detection of the expression of M2-type anti-inflammatory factors ($n = 4$ samples/group for B and C panels). (D) Flow cytometry to detect phagocytosis of microglia. (E, F) Fluorescence microscopy to observe FITC inside microglia, and fluorescence quantification. (G) The migration and invasion of BV2 cells. (H) The wound closure area was measured by the Image J software. (I) The number of invaded cells was counted by cell counter of Image J software ($n = 3$ independent experiments for D−I panels). Data are mean ± SEM; $^{*}P < 0.05$, $^{**}P < 0.01$, $^{***}P < 0.001$.

staining. (C) Fluorescence quantification of NeuN staining. (D) Quantification of synaptic spine density ($n = 5$ images/group for A−D panels). (E) Western blot detects the expression of MAP2 and PSD95 in brain tissue. (F, G) Quantification of MAP2 and PSD95. (H) Western blot detects the expression of inflammatory factors TNF-α and IL-1β in brain tissue. (I, J) Quantification of TNF-α and IL-1β in panel G, respectively ($n = 3$ samples/group for E−J panels). Data are mean ± SEM; $^{**}P < 0.01$, $^{***}P < 0.001$.

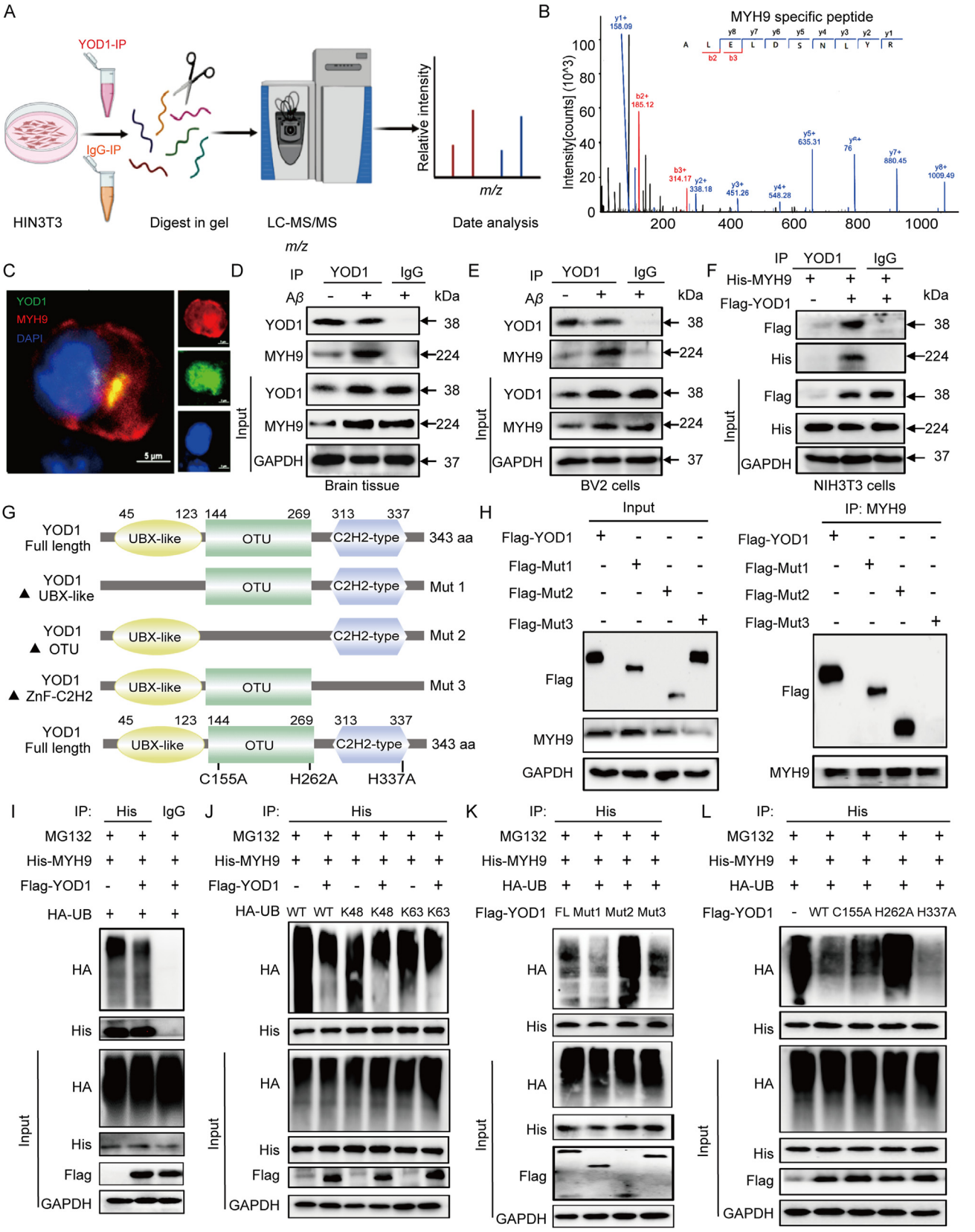

Figure 7 YOD1 C-terminal Znf domain binds to MYH9 and affects MYH9 ubiquitination through H262A. (A) Schematic illustration of YOD1-IP and IgG-IP proteome screening. (B) MS spectrum of MYH9 peptide. (C) ICC detection of co-localization of MYH9 and YOD1 in microglia (D) Co-IP analysis of YOD1-MYH9 interaction in brain tissue. (E) Co-IP analysis of YOD1-MYH9 interaction in BV2 cells. (F) Co-IP analysis tool for YOD1-MYH9 interaction in NIH/3T3 cells. (G) Schematic of YOD1 structures and three different truncated constructs tagged

regulation of AD pathology[37]. However, these studies mostly focused on the function of DUBs in neuronal cells. In recent years, some inflammation-related DUBs are gradually been discovered[38]. For example, USP18 is identified as a regulatory molecule that prevents aberrant activation of microglia[39]. USP19 regulates NLRP3 function through autophagy to suppress inflammation and promote M2-like macrophage polarization. Deletion of A20 specifically in microglia renders mice hypersensitive to autoimmune encephalomyelitis due to increased proinflammatory gene production resulting from augmented activation of the NLRP3 inflammasome[40]. These led to the identification of novel molecular mechanisms of inflammation-related DUB function, allowing the development of specific DUB inhibitors/agonists to treat diseases[41]. In this study, we found that deubiquitinase YOD1 is highly expressed in microglia in different AD models. Knocking out microglia YOD1 can significantly reduce the levels of inflammatory cytokines, prevent abnormal migration and phagocytosis of microglia, and improve the pathology of AD. We also used an Aβ-induced acute AD model to demonstrate that YOD1 is also involved in Aβ-induced acute AD pathology. Together, the role of YOD1 in improving AD pathology by affecting microglia homeostasis has been confirmed.

As we know, the role and function of DUB are closely related to substrate proteins. As a deubiquitinase, YOD1 can affect the stability or activation of target proteins by regulating their ubiquitin levels. Here, we identified MYH9 as a substrate of YOD1 through LC−MS/MS analysis. MYH9 protein is a member of the myosin II subfamily and plays an important regulatory role in the remodeling of the membrane and cytoskeleton necessary for the performance of functions that characterize activated microglia, such as polarization, migration, and phagocytosis[29,42]. MYH9 has been shown to play an important role in microglial polarization. M1 microglia are characterized by an amoeba shape, high mobility, and strong phagocytic ability, producing pro-inflammatory mediators such as IL-6, IL-1β, and tumor necrosis factor-α (TNF-α); in contrast, M2 microglia are characterized by a typical elongated morphology, branching processes, and releasing anti-inflammatory molecules, such as IL-4, IL-10[43-45]. Inhibiting the expression of MYH9 can inhibit the activation of M1 pro-inflammatory microglia and exert a neuroprotective effect[46,47]. For example, high arginine inhibited MYH9 from changing the spatial structure of the actin cytoskeleton on the surface of T cells, promoting the growth of filopodia, inhibiting the migration and proliferation of T cells, and alleviating the progression of atherosclerosis[48]. During phagocytic clearance, MYH9 is also redistributed and co-localizes with cargo from ingested cellular debris, promoting phagocytosis[49]. In this study, we showed that YOD1 can bind to MYH9 *via* its C2H2-type domain. After MYH9 is knocked down, YOD1's regulation of microglial migration and phagocytosis is weakened. In addition, the inflammatory response and nerve cell damage in MYH9-knocked down microglia are improved. It is suggested that MYH9 may serve as a direct substrate of YOD1 to regulate the phagocytic, migration, and polarization functions of microglia in AD.

YOD1 was reported as a specific DUB to hydrolyze the K48- and K63-linked poly-ubiquitin chains from different substrate proteins[50,51]. Here, we show that YOD1 removes K48-linked polyubiquitin chains from MYH9, thereby blocking MYH9 degradation by the proteasome. MYH9 is widely distributed in vascular endothelial cells, macrophages, fibroblasts, T cells, neutrophils, and other cells[52,53]. Research has confirmed that MYH9 is closely related to cell adhesion and migration, cytokinesis, transport of organelles and particles, tumor metastasis, cardiovascular and cerebrovascular processes, etc., indicating that MYH9 is a functional protein closely related to physiological and pathological processes. In recent years, some MYH9 inhibitors have been developed, such as blebbistatin, a specific inhibitor of MYH9, which can dose-dependently block cell movement, inhibit the metastasis and invasion of cancer cells, and reduce the occurrence of glaucoma[54]. However, potential toxicity and off-target effects limit their applications. In this study, we promoted the degradation of MYH9 protein by targeting the key regulator YOD1 to effectively avoid off-target effects. Therefore, targeting YOD1 may provide new strategies for the treatment of MYH9-related diseases.

A limitation of this study is that we did not use microglia-specific YOD1 knockout mice to elucidate the role of YOD1 in regulating migration, phagocytosis, and inflammation. However, we achieved the purpose of specifically knocking out microglia YOD1 in 3 × Tg mice by injecting an AAV virus into the hippocampus of 3 × Tg mice, which also clarified our conclusion. However, the function of YOD1 in other cells and its effect on Tau pathology still need to be further explored. In addition, the other potential interacting proteins that interact with YOD1 do not match the role of YOD1 or have not been reported to be related to AD pathology. For example: RPLP2 encodes 60S acidic ribosomal protein P2 protein, regulates liver cancer cell proliferation[55] and its role in AD is still unclear. The eEF1A1 protein is a novel prognostic biomarker and potential therapeutic target for HCC patients[56]. ACTB is one of the nonmuscle cytoskeletal actins that are involved in cell motility, structure, and integrity, which has been shown to regulate NO production[57]. MYL6 encodes myosin light chain polypeptide 6 protein, which is a hexameric ATPase cell movement protein[58]. But its function in AD is still unclear. Nevertheless, we cannot completely rule out the possibility that other substrates mediate the effects of YOD1, which is worth exploring in the future. Last but not least, it would be a crucial step to explore how Aβ stimulates YOD1 expression, so further investigation on the transcription regulation of YOD1 is needed in the future.

with FLAG (UBXL, OTUD, Znf) and the three key sites in the active center of the enzyme, cysteine at position 155, histidine at position 262 and histidine at position 337 were designed. (H) Co-IP analysis of the binding region of MYH9 and YOD1. (I) His-MYH9, HA-UB, and Flag-YOD1 overexpression plasmids were co-transfected into NIH/3T3 cells, and MYH9 ubiquitination was detected by immunoblotting using His-specific antibodies. (J) Co-transfection of His-MYH9, HA-UB, HA-K48, HA-K63, and Flag-YOD1 overexpression plasmids into NIH/3T3 cells. YOD1-regulated MYH9 ubiquitination pattern was detected by immunoblotting with His-specific antibodies. (K) Different segments of YOD1, His-MYH9 and HA-UB overexpression plasmids were co-transfected into NIH/3T3 cells, and the effect of YOD1 segments on MYH9 ubiquitination was detected by Co-IP. (L) Overexpression plasmids of the active sites of His-MYH9, HA-UB and Flag-YOD1 were co-transfected into NIH/3T3 cells. The active site of YOD1 regulating MYH9 ubiquitination was detected by immunoblotting using His-specific antibodies. $n = 3$ independent experiments for all panels.

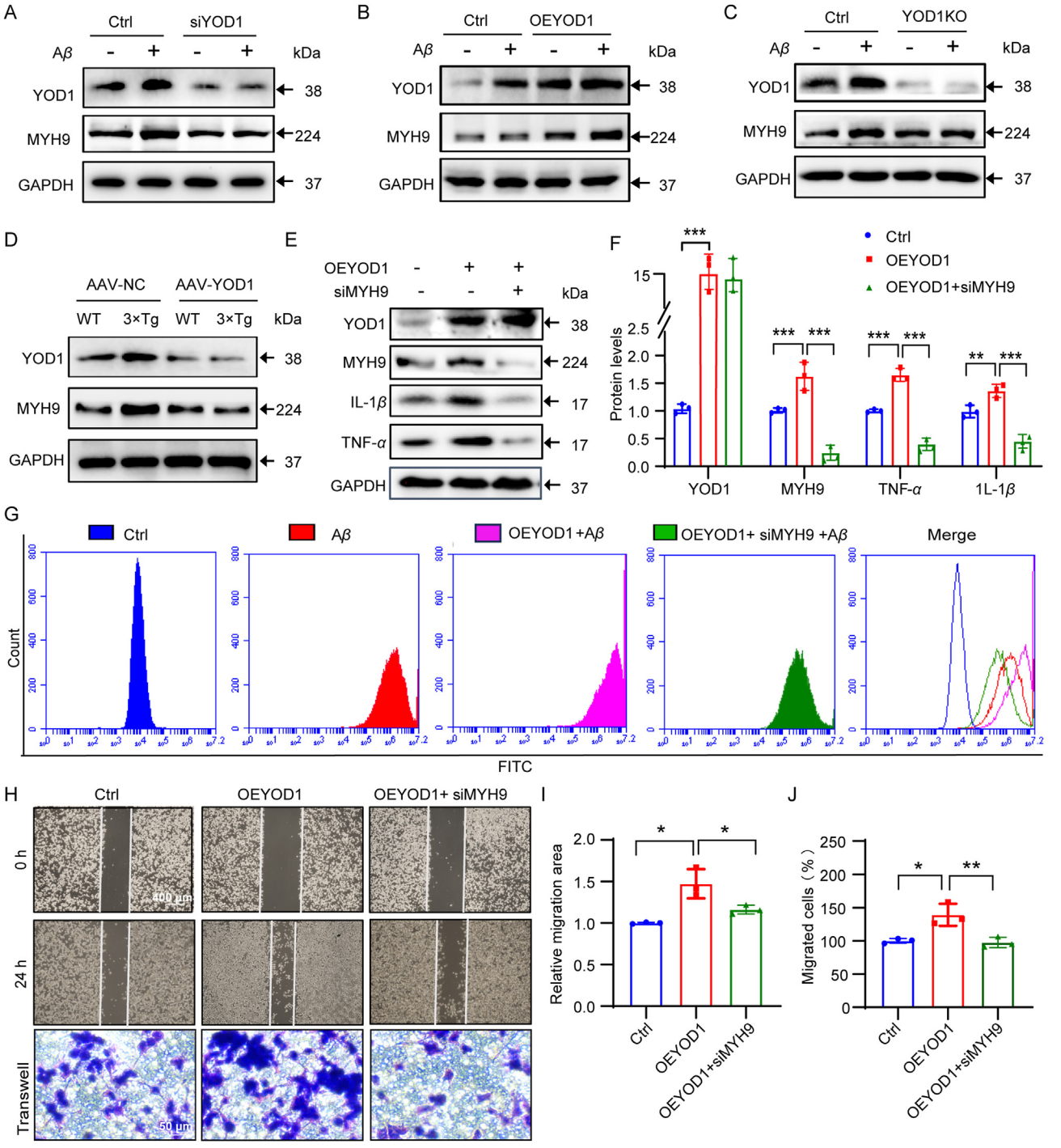

Figure 8 YOD1 improves Aβ-induced microglial migration, phagocytosis and inflammatory response by regulating MYH9. (A) Western blot detects the effect of YOD1 silencing on MYH9 protein levels in microglia. (B) Western blot detects the effect of YOD1 overexpression on MYH9 protein levels in microglia. (C) Western blot detects the effect of YOD1 knockout on MYH9 protein levels in brain tissue of Aβ-infusion mode mice. (D) Western blot detects the effect of YOD1 knockout on MYH9 protein levels in brain tissue of 3 × Tg model mice. (E, F) The expression of inflammatory factors is reduced after MYH9 knockdown in microglia. (G) Microglial phagocytosis function is reduced after MYH9 knockdown in microglia. (H–J) The migration function of microglia is reduced after MYH9 knockdown in microglia. Data are man ± SEM, $n = 3$ independent experiments for all panels; $^{*}P < 0.05$, $^{**}P < 0.01$, $^{***}P < 0.001$.

5. Conclusions

We demonstrate that YOD1 deubiquitinates MYH9, enhances MYH9 stability, and regulates microglial migration, phagocytosis, and inflammation regulation functions. These findings deepen our understanding of the role of DUBs in microglia and provide a basis for targeting YOD1 for AD therapy.

Acknowledgements

This study was supported by the National Natural Science Foundation of China (21961142009 to Guang Liang and 82360805 to Jinfeng Sun), Zhejiang Provincial Key Scientific Project (2021C03041 to Guang Liang), Natural Science Foundation of Zhejiang province (LQ23H090018 to Xia Zhao) and Medical and health Science and Technology Project of Zhejiang Province (2024KY055 to Xia Zhao).

Author contributions

Jinfeng Sun: Visualization, Formal analysis, Data curation. Fan Chen: Data curation. Lingyu She: Data curation. Yuqing Zeng: Data curation. Hao Tang: Data curation. Bozhi Ye: Formal analysis. Wenhua Zheng: Methodology. Li Xiong: Data curation. Liwei Li: Data curation. Luyao Li: Data curation. Qin Yu: Software. Linjie Chen: Software. Wei Wang: Writing − review & editing. Guang Liang: Writing − review & editing, Supervision, Resources, Funding acquisition, Conceptualization. Xia Zhao: Writing − original draft, Visualization, Funding acquisition, Data curation, Conceptualization.

Conflicts of interest

The authors declare no conflicts of interest.

Appendix A. Supporting information

Supporting information to this article can be found online at https://doi.org/10.1016/j.apsb.2024.11.020.

References

1. Wake H, Moorhouse AJ, Nabekura J. Functions of microglia in the central nervous system—beyond the immune response. *Neuron Glia Biol* 2011;**7**:47−53.
2. Colonna M, Butovsky O. Microglia function in the central nervous system during health and neurodegeneration. *Ann Rev Immunol* 2017;**35**:441−68.
3. Schwartzentruber J, Cooper S, Liu JZ, Barrio-Hernandez I, Bello E, Kumasaka N, et al. Genome-wide meta-analysis, fine-mapping and integrative prioritization implicate new Alzheimer's disease risk genes. *Nat Genet* 2021;**53**:392−402.
4. Gulen MF, Samson N, Keller A, Schwabenland M, Liu C, Glück S, et al. cGAS−STING drives ageing-related inflammation and neurodegeneration. *Nature* 2023;**620**:374−80.
5. Chowen JA, Garcia-Segura LM. Microglia, neurodegeneration and loss of neuroendocrine control. *Prog Neurobiol* 2020;**184**:101720.
6. Subbarayan MS, Joly-Amado A, Bickford PC, Nash KR. CX3CL1/CX3CR1 signaling targets for the treatment of neurodegenerative diseases. *Pharmacol Ther* 2022;**231**:107989.
7. Gómez Morillas A, Besson VC, Lerouet D. Microglia and neuroinflammation: what place for P2RY12?. *Int J Mol Sci* 2021;**22**:1636.
8. Deng Z, Dong Y, Zhou X, Lu JH, Yue Z. Pharmacological modulation of autophagy for Alzheimer's disease therapy: opportunities and obstacles. *Acta Pharm Sin B* 2022;**12**:1688−706.
9. Çetin G, Klafack S, Studencka-Turski M, Krüger E, Ebstein F. The ubiquitin−proteasome system in immune cells. *Biomolecules* 2021;**11**:60.
10. Amerik AY, Hochstrasser M. Mechanism and function of deubiquitinating enzymes. *Biochim Biophys Acta* 2004;**1695**:189−207.
11. Wei Z, Zeng K, Hu J, Li X, Huang F, Zhang B, et al. USP10 deubiquitinates Tau, mediating its aggregation. *Cell Death Dis* 2022;**13**:726.
12. Zheng Q, Li G, Wang S, Zhou Y, Liu K, Gao Y, et al. Trisomy 21-induced dysregulation of microglial homeostasis in Alzheimer's brains is mediated by USP25. *Sci Adv* 2021;**7**:eabe1340.
13. Zheng Q, Song B, Li G, Cai F, Wu M, Zhao Y, et al. USP25 inhibition ameliorates Alzheimer's pathology through the regulation of APP processing and Aβ generation. *J Clin Invest* 2022;**132**:e152170.
14. Xu J, Yu T, Pietronigro EC, Yuan J, Arioli J, Pei Y, et al. Peli1 impairs microglial Aβ phagocytosis through promoting C/EBPβ degradation. *PLoS Biol* 2020;**18**:e3000837.
15. Shao X, Chen Y, Wang W, Du W, Zhang X, Cai M, et al. Blockade of deubiquitinase YOD1 degrades oncogenic PML/RARα and eradicates acute promyelocytic leukemia cells. *Acta Pharm Sin B* 2022;**12**:1856−70.
16. Park JH, Kim SY, Cho HJ, Lee SY, Baek KH. YOD1 Deubiquitinates NEDD4 involved in the Hippo signaling pathway. *Cell Physiol Biochem* 2020;**54**:1−14.
17. Wu Y, Duan Y, Han W, Cao J, Ye B, Chen P, et al. Deubiquitinase YOD1 suppresses tumor progression by stabilizing E3 ligase TRIM33 in head and neck squamous cell carcinoma. *Cell Death Dis* 2023;**14**:517.
18. Tanji K, Mori F, Miki Y, Utsumi J, Sasaki H, Kakita A, et al. YOD1 attenuates neurogenic proteotoxicity through its deubiquitinating activity. *Neurobiol Dis* 2018;**112**:14−23.
19. Schimmack G, Schorpp K, Kutzner K, Gehring T, Brenke JK, Hadian K, et al. YOD1/TRAF6 association balances p62-dependent IL-1 signaling to NF-κB. *Elife* 2017;**6**:e22416.
20. Zhao X, Sun J, Xiong L, She L, Li L, Tang H, et al. β-Amyloid binds to microglia Dectin-1 to induce inflammatory response in the pathogenesis of Alzheimer's disease. *Int J Biol Sci* 2023;**19**:3249−65.
21. Cai Y, Liu J, Wang B, Sun M, Yang H. Microglia in the neuroinflammatory pathogenesis of Alzheimer's disease and related therapeutic targets. *Front Immunol* 2022;**13**:856376.
22. Butler CA, Popescu AS, Kitchener EJA, Allendorf DH, Puigdellívol M, Brown GC. Microglial phagocytosis of neurons in neurodegeneration, and its regulation. *J Neurochem* 2021;**158**:621−39.
23. Yu F, Wang Y, Stetler AR, Leak RK, Hu X, Chen J. Phagocytic microglia and macrophages in brain injury and repair. *CNS Neurosci Ther* 2022;**28**:1279−93.
24. Subhramanyam CS, Wang C, Hu Q, Dheen ST. Microglia-mediated neuroinflammation in neurodegenerative diseases. *Semin Cell Dev Biol* 2019;**94**:112−20.
25. Zhao X, Huang X, Yang C, Jiang Y, Zhou W, Zheng W. Artemisinin attenuates Amyloid-induced brain inflammation and memory impairments by modulating TLR4/NF-κB signaling. *Int J Mol Sci* 2022;**23**:6354.
26. Li Y, Reverter D. Molecular mechanisms of DUBs regulation in signaling and disease. *Int J Mol Sci* 2021;**22**:986.
27. Harrigan JA, Jacq X, Martin NM, Jackson SP. Deubiquitylating enzymes and drug discovery: emerging opportunities. *Nat Rev Drug Discov* 2018;**17**:57−78.
28. Reville K, Crean JK, Vivers S, Dransfield I, Godson C. Lipoxin A4 redistributes myosin IIA and Cdc42 in macrophages: implications for phagocytosis of apoptotic leukocytes. *J Immunol* 2006;**176**:1878−88.
29. Porro C, Pennella A, Panaro MA, Trotta T. Functional role of non-muscle myosin II in microglia: an updated review. *Inte J Mol Sci* 2021;**22**:6687.
30. He C, Li Z, Yang M, Yu W, Luo R, Zhou J, et al. Non-coding RNA in microglia activation and neuroinflammation in Alzheimer's disease. *J Inflamm Res* 2023;**16**:4165−211.
31. Gao X, Cao Z, Tan H, Li P, Su W, Wan T, et al. LncRNA, an emerging approach for neurological diseases treatment by regulating microglia polarization. *Front Neurosci* 2022;**16**:903472.
32. Han Z, Jia Q, Zhang J, Chen M, Wang L, Tong K, et al. Deubiquitylase YOD1 regulates CDK1 stability and drives triple-negative breast cancer tumorigenesis. *J Exp Clin Cancer Res* 2023;**42**:228.
33. Saitgareeva AR, Bulygin KV, Gareev IF, Beylerli OA, Akhmadeeva LR. The role of microglia in the development of neurodegeneration. *Neurol Sci* 2020;**41**:3609−15.

34. Wang D, Gu X, Ma X, Chen J, Zhang Q, Yu Z, et al. Nanopolyphenol rejuvenates microglial surveillance of multiple misfolded proteins through metabolic reprogramming. *Acta Pharm Sin B* 2023;**13**:834−51.
35. Tzioras M, McGeachan RI, Durrant CS, Spires-Jones TL. Synaptic degeneration in Alzheimer disease. *Nat Rev Neurol* 2023;**19**:19−38.
36. Arendt T. Synaptic degeneration in Alzheimer's disease. *Acta Neuropathol* 2009;**118**:167−79.
37. Lee JH, Shin SK, Jiang Y, Choi WH, Hong C, Kim DE, et al. Facilitated Tau degradation by USP14 aptamers *via* enhanced proteasome activity. *Sci Rep* 2015;**5**:10757.
38. Li L, Wei J, Li S, Jacko AM, Weathington NM, Mallampalli RK, et al. The deubiquitinase USP13 stabilizes the anti-inflammatory receptor IL-1R8/Sigirr to suppress lung inflammation. *EBioMed* 2019;**45**:553−62.
39. Liu B, Ruan J, Chen M, Li Z, Manjengwa G, Schlüter D, et al. Deubiquitinating enzymes (DUBs): decipher underlying basis of neurodegenerative diseases. *Mol Psychiatry* 2022;**27**:259−68.
40. Ruan J, Schlüter D, Wang X. Deubiquitinating enzymes (DUBs): DoUBle-edged swords in CNS autoimmunity. *J Neuroinflammation* 2020;**17**:102.
41. Schauer NJ, Magin RS, Liu X, Doherty LM, Buhrlage SJ. Advances in discovering deubiquitinating enzyme (DUB) inhibitors. *J Med Chem* 2020;**63**:2731−50.
42. Pecci A, Ma X, Savoia A, Adelstein RS. MYH9: structure, functions and role of non-muscle myosin IIA in human disease. *Gene* 2018;**664**:152−67.
43. Du L, Zhang Y, Chen Y, Zhu J, Yang Y, Zhang HL. Role of microglia in neurological disorders and their potentials as a therapeutic target. *Mol Neurobiol* 2017;**54**:7567−84.
44. Michell-Robinson MA, Touil H, Healy LM, Owen DR, Durafourt BA, Bar-Or A, et al. Roles of microglia in brain development, tissue maintenance and repair. *Brain* 2015;**138**:1138−59.
45. Lyu J, Xie D, Bhatia TN, Leak RK, Hu X, Jiang X. Microglial/macrophage polarization and function in brain injury and repair after stroke. *CNS Neurosci Ther* 2021;**27**:515−27.
46. Yang K, Zhang Z, Liu X, Wang T, Jia Z, Li X, et al. Identification of hypoxia-related genes and exploration of their relationship with immune cells in ischemic stroke. *Sci Rep* 2023;**13**:10570.
47. Pan D, Liu W, Zhu S, Fan B, Yu N, Ning G, et al. Potential of different cells-derived exosomal microRNA cargos for treating spinal cord injury. *J Orthop Translat* 2021;**31**:33−40.
48. Nitz K, Lacy M, Bianchini M, Wichapong K, Kücükgöze IA, Bonfiglio CA, et al. The amino acid homoarginine inhibits atherogenesis by modulating T-Cell function. *Circ Res* 2022;**131**:701−12.
49. Caberoy NB, Alvarado G, Li W. Tubby regulates microglial phagocytosis through MerTK. *J Neuroimmunol* 2012;**252**:40−8.
50. Ritorto MS, Ewan R, Perez-Oliva AB, Knebel A, Buhrlage SJ, Wightman M, et al. Screening of DUB activity and specificity by MALDI-TOF mass spectrometry. *Nat Commun* 2014;**5**:4763.
51. Zhu J, Pittman S, Dhavale D, French R, Patterson JN, Kaleelurrrahuman MS, et al. VCP suppresses proteopathic seeding in neurons. *Mol Neurodegener* 2022;**17**:30.
52. Asensio-Juárez G, Llorente-González C, Vicente-Manzanares MJC. Linking the landscape of MYH9-related diseases to the molecular mechanisms that control non-muscle myosin II-A function in cells. *Cells* 2020;**9**:1458.
53. Li Y, Friedmann DR, Mhatre AN, Lalwani AK. MYH9-siRNA and MYH9 mutant alleles: expression in cultured cell lines and their effects upon cell structure and function. *Cell Motil Cytoskeleton* 2008;**65**:393−405.
54. Mikulich A, Kavaliauskiene S, Juzenas P. Blebbistatin, a myosin inhibitor, is phototoxic to human cancer cells under exposure to blue light. *Biochim Biophys Acta* 2012;**1820**:870−7.
55. Guo J, Huang M, Deng S, Wang H, Wang Z, Yan B. Highly expressed RPLP2 inhibits ferroptosis to promote hepatocellular carcinoma progression and predicts poor prognosis. *Cancer Cell Int* 2023;**23**:278.
56. Chen SL, Lu SX, Liu LL, Wang CH, Yang X, Zhang ZY, et al. eEF1A1 overexpression enhances tumor progression and indicates poor prognosis in hepatocellular carcinoma. *Transl Oncol* 2018;**11**:125−31.
57. Zhang X, Wei M, Fan J, Yan W, Zha X, Song H, et al. Ischemia-induced upregulation of autophagy preludes dysfunctional lysosomal storage and associated synaptic impairments in neurons. *Autophagy* 2021;**17**:1519−42.
58. Xu Z, Zhou Y, Yu H, Chen X, Ma YQ. Myosin light chain 6 (Myl6) interacts with kindlin-3 and is required to support integrin αIIbβ3 activation in platelets in mice. *J Thromb Haemost* 2024;**22**:2009−17.